DOI: 10.2195/lj_NotRev_kuehner_en_201803_01
URN: urn:nbn:de:0009-14-46707

Assessment of damage behavior of twisted ropeway ropes in operation

Konstantin Kuehner
Karl-Heinz Wehking

Jakob AG, Schweiz
Institute of Mechanical Handling and Logistics (IFT)
University of Stuttgart

Wire ropes naturally build up torque and twist under tension or while running over sheaves. Within operation of rope drives, the twist is massaged through different rope sections and remains in specific areas, changing the ropes basic geometry. This leads to vibration, wear and a reduced rope lifetime. Former research projects could identify a relation between the dimension of twist and the rope bending cycles until failure in laboratory tests, but it was neither possible to predict the expectable amount of twist in an existing installation nor to evaluate how many rotations of a rope in operation will lead to a specific amount of twist. A funded two-years research project dealt with twist initiators, their quantitative effects and the fatigue-life of twisted ropeway-ropes. The project followed three basic topics:

- **Bending tests on twisted langslay ropes generating additional lifetime factors of Feyrer's formula**
- **Theoretic investigation on quantity of influences of mechanic twist initiators, using FMEA of relevant parameters. Comparison of rotation theory and measurements on existing ropeways with an innovative rotation sensor-system.**
- **Rope lay length analysis by filtered magnetoinductive rope test signals of almost discarded haulingropes identifying the storage of twist in jigback tramways.**

The results were combined to a final model allowing to predict rotation and twist storage by design parameters as well as to quantify effects on ropes lifetime.

[Keywords: steel wire ropes; ropeways; endurance; damage behavior; rotation; twist]

1 INTRODUCTION

1.1 ROPEWAYS

Ropeway systems represent a modern still upcoming means of transportation. Statistic figures collected by the ITTAB (International Meeting of Technical Authorities for Cableways) in 2015 indicate a world-wide number of rides of 6.2 Billion passengers using about 22,000 ropeway installations [ITT15]. The core element of a ropeway is the steel wire rope itself, as it is directly influencing the ropeways safety, availability and economic efficiency. Investing for a new rope can be compared to about 5 to 10 % of the entire initial costs of a modern ropeway (see fig. 1).

Figure 1. Modern ropeway system

1.2 TWIST IN ROPEWAY ROPES

In every setup of rope drive, the running rope rotates around its axis due to load changes and dynamics as well as by mechanical contact to sheaves, rollers and drums or static guiding elements [Opl04]. Assuming an ideal line setup without fleet angle, this rotation is created both by the spring-like wire- and strand-layout of the rope, leading to inner torque under load, and by the screw-like surface shape of at least classic stranded ropes. Depending on the arrangement of rope driving- and guiding elements in an individual installation, this rotation can be massaged through the rope and stored at discrete sections, leading to

DOI: 10.2195/lj_NotRev_kuehner_en_201803_01
URN: urn:nbn:de:0009-14-46707

rope twist which causes a local change of the original lay length [Eng94]. A deviation of lay length can lead to inner touching of the strands which can increase the damage development of the rope severely [Bri95]. Rope twist is differentiated between a de-twisted rope to an increased lay length by negative specific twist angle "-ω" and closing twist which leads to a reduced lay length, specified by a positive twist angle "+ω" [Ern12],[Web13]. Figures 2 and 3 shows different states of twist illustrated by a soft hand model.

Figure 2. Hand model showing closing twist "+ω"

Figure 3. Hand model showing de-twisting "-ω" (right)

Up to now, some parameters have been investigated to predict the lifetime of specific ropes designs in twisted state, but still there are rope constructions which have not been in focus of research yet. Furthermore, it is not known at all how much rotation is created by specific rope drive elements, how much twist will be stored in summary and how much lifetime reduction has to be expected. After successful trials using a new digital rotation sensor [Weh13], a publicly funded project was launched[1], consisting of three focal points, which are illustrated by figure 4. The investigated ropes are mainly running ropes of ropeways which allow access to big scale rope drives and their related rotation behavior. Later on, methods of transferring the results to general rope drives are discussed and approaches are given.

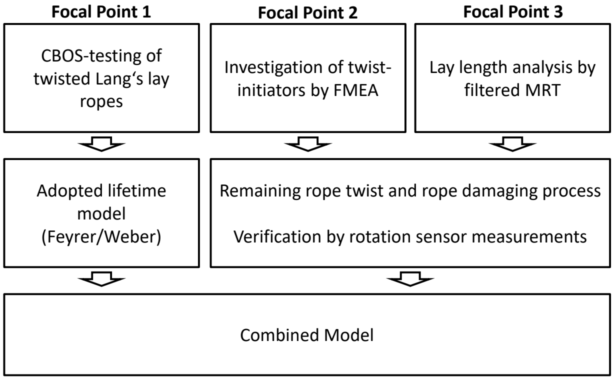

Figure 4. Illustration of research project structure investigating the chain from rotation over stored twist to expectable lifetime reduction of a running (ropeway) ropes

2 CBOS-Testing of twisted Lang's lay ropes and lifetime calculation

Within the project, two CBOS[2]-test series at different load levels were carried out to enlarge the database of [Web13] to the rope-designs of Lang's lay ropes with fiber core. The rope samples are twisted to a defined level referred to a reference length of 100 times rope diameter. By performing repetitive tests at each twist angle level, the values can be approximated by regression to a compensating curve. The diagram in figure 6 shows the results for bending tests at a diameter-ratio of sheave-diameter to rope diameter of D/d=20 and a diameter-related rope tension of $S/d^2=100\ N/mm^2$. The rope used in the tests was of the type 15 6x19S-FC 1960 B zZ, see figure 5. The continuous best-fit curve relates to the achieved bending cycles N until rope failure, the dashed one shows the approximated average point of discard NA[3] by visual inspection.

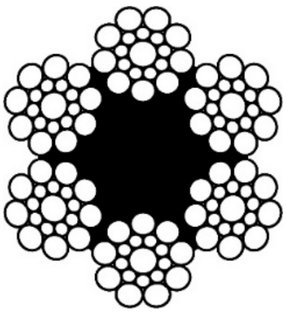

Figure 5. Example of a ropeway rope type 6x19 Seale

[1] German Research Foundation DFG, project no. WE 2187/36-1

[2] Continuous bending over sheaves

[3] Abbreviation „A" for german „Ablegereife", meaning discard maturity

DOI: 10.2195/lj_NotRev_kuehner_en_201803_01
URN: urn:nbn:de:0009-14-46707

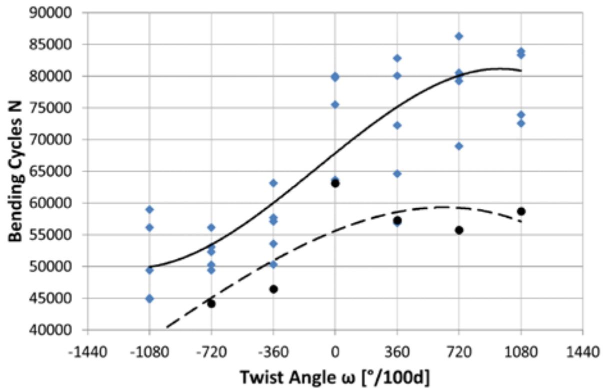

Figure 6. Bending test results at D/d=20, S/d²=100 N/mm² (continuous line – point of rope failure; dashed line – point of discard by visual inspection)

The results show clearly, that in de-twisted state respectively at a long lay length, the rope lifetime until break is massively reduced while at closing twist, the rope lifetime increases slightly or stays constant. This can be explained first by the amount of strands touching a sheave and the resulting pressure distribution in relation to the actual lay length of a rope. Second, the rope compound is weakened against transverse forces as the wire tension is reduced at decreasing lay angles. This is enlarging the tendency of the rope to ovalize which leads to an increased damage behavior. Even stronger, the time slot between visible discard maturity and total rope failure is reduced by negative twist angles displayed in the diagram. To investigate the inner damage caused by a de-twisted lay length, a suitable bending test setup was stopped in advance of its expected failure to open it into strands and carry out a microscopic analysis. The strands show inner abrasion at their touching zones and incipient cracks leading to inner wire breaks.

This behavior is directly related to a reduced safety level as de-twisted Lang's lay ropes develop more increased inner damage level than their outer appearance may indicate. Even under magneto-inductive supervision at usually 3 year intervals [DIN12927], intermediate visual inspections may lead to euphemized evaluations.

To fit to the large diameter ratios of ropeways which have to be minimum D/d=80, the polynomic structure of [Web13],[Fey00] was modified to a final formula fulfilling the recommendations about standard deviation and coefficient of determination.

$$\lg N_\omega = a_0 + \left(a_1 + a_3 \cdot \lg\frac{D}{d}\right)\left(\lg\frac{S}{d^2} - 0{,}4 \cdot \lg\frac{R_0}{1770}\right)$$

$$+a_2 \cdot \lg\frac{D}{d} + \lg f_d + \lg f_l$$

$$+b_0 \cdot \left(\frac{\omega}{\frac{Sd_0^2}{d^2 S_0}}\right) + b_1 \cdot \left(\frac{\omega}{\frac{Sd_0^2}{d^2 S_0}}\right)^2 + b_2 \cdot \left(\frac{\omega}{\frac{Sd_0^2}{d^2 S_0}}\right)^3$$

N_ω	gainable bending cycles in twisted state
D	sheave diameter [mm]
d	rope diameter [mm]
S	rope force [N]
a_i, b_i & f_i	factors for rope lifetime calculation
ω	twist angle [rad/100*d]
R_0	rope nominal strength [N/mm²]
S_0, d_0	auxiliary factors clearing dimensions of "S/d²"

The final factors b0 to b2 for calculating the point of discard, indicated by (A), and rope breakage are given in the following table 1.

Table 1. Constant factors calculated by the test results for rope type 6x19S-FC zZ referring to discard (A) and breakage

Constant factors	**b0(A)**	**b1(A)**	**b2(A)**
Discard	0.8022	-2.5351	-6.1300
Constant factors	**b0**	**b1**	**b2**
rope breakage	0.8018	-1.7440	-9.4568

3 Investigation of potential Twist-Initiators by FMEA

The method of FMEA[4] is well-approved in the industrial environment to avoid planning, concept and design failures at prototype stage of new developments [Ebe13]. The method consists of several main steps:

- Step 1: Structural analysis
- Step 2: Functional analysis / Failure analysis
- Step 3: Risk evaluation
- Step 4: Measures of Improvement

Although the analysis of rope twist is not a product development process, the method provides valuable features to capture the complex system of a ropeway installation, combining structural analysis with the knowledge of both experts and open-minded participants with technical understanding.

After the structural analysis of step 1 of the FMEA, illustrating all mechanical elements of a ropeway installation which are directly linked to rope forces, friction and related rotation and twist, in step 2, functions and potential

[4] Failure Mode and Effekt Analysis

DOI: 10.2195/lj_NotRev_kuehner_en_201803_01
URN: urn:nbn:de:0009-14-46707

failures are listed and linked to every structural element in function- and failure-nets. To every failure, three characteristics – severity, probability & detection – are evaluated by a scoring system to classify its individual risk level, forming a final "risk priority number", shortly called RPN. Following the failure net, it is possible to identify the main failures which lead to the heaviest impact. Therefore, usually a subsequent Pareto-analysis, also known as the 80-20-rule, is performed to determine the minority of failures which cause the majority of effects. Table 2 shows the final 14 elements which lead to rope twist according to the result of the FMEA on twist in ropeway installations.

Table 2. Main elements leading to rope twist according to the result of the FMEA

No.	Failure description	RPN
01	Difference in load level by rope weight (height stresses)	1000
02	Change in rope force by running direction up-/downhill	1000
03	Loss by elastic deformation	1000
04	Loss by elastic deformation	1000
05	Change of rope force by traction drive	1000
06	Change of rope force by acceleration / deceleration	1000
07	Frictional loss at roller (insufficient amount of rollers)	1000
08	Frictional loss at roller	1000
09	Frictional loss at roller	1000
10	Insufficient Lubrication	640
11	Low Modulus of Elasticity (rope appears "soft")	560
12	Radial run-out	560
13	Slack / soft to twist	500
14	High normal force	400

For every determined type of influencing element, a mechanical and/or mathematical background is established to allow either a calculation of the resulting rope torque caused by the individual element or to at least quantify the severity of its influence in relation to the acting boundary parameters. The analysis finally allows pre-calculating an expectable rope torque in the ropeway installation. As most of the twist factors are influenced by only a few parameters like the geometrical line of the ropeway, location of drive and tensioning elements, the cabin size or the rope design and diameter, the analysis can be automated using a simplified master data sheet and e.g. Microsoft Excel as processing software, which can be easily filled out by planners, developers or operators.

The rotation measurement on hauling and counter ropes of 25 ropeway systems of the type "jigback" aerial tramway was carried out (see figure 7). The measurements are used to validate both assumptions and theoretical analysis as well as to complement the physical backgrounds of rope rotation.

Figure 7. Digital rotation measurement at a jigback aerial tramway

The database of measurements allows first general statements on the rotation behavior of hauling ropes:

- The rotational behavior of the hauling ropes is reproducible. By carrying out measurements repeatedly in the same set-ups, it could be proved that rope rotation is a physical process rarely influenced by accidental impacts.
- Similar line setups show similar rotational behavior. Comparing several measurements, similar geometrical arrangements of different ropeway installations generate similar curve shapes. The amount of rotation may vary over the height and length of the installation, but the curve shapes are basically the same.
- Ropes show the same rotational behavior under similar boundary conditions. By measuring two parallel hauling ropes in the same ropeway system at the same time, it could be proved that these ropes rotate parallel in the same way and amount.
- Tower rollers create both a twist barrier and rope torque. Following the measurement charts, most ropes show a characteristic rotation gradient linked to the passage of both car and sensor passing a tower. The rope rotates following height stresses and twist compensation between

DOI: 10.2195/lj_NotRev_kuehner_en_201803_01
URN: urn:nbn:de:0009-14-46707

the field spans at these points. A sketch in Figure 5 explains the rope rotation behavior above the car within a downhill ride for a right hand laid rope.

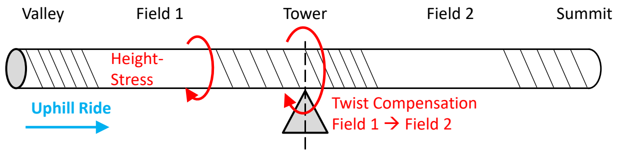

Figure 8. Rope rotation behavior above the car within a downhill ride for a right hand laid rope

The amount of rotation, twist storage and twist release is directly linked to the field geometry, the roller pressure and friction loss due to rubber linings on the towers. The final model combines the severity of influencing factors and their impact to the observed rope rotation, residual change of lay length and finally to the loss of effective rope lifetime.

To get an impression of typical amounts of rope rotation within one ride of a single track rope system, the following table 3 gives extreme and average values, measured in a distance of 100m to the cabin.

Table 3. Average and extreme values of rope rotation of jigback tramways with single track ropes, measured in 100m distance to the cabin (positive: closing twist, negative: de-twisting)

1 track rope without slack hangers	**Upper hauling rope Uphill ride**	**Upper hauling rope Downhill ride**	**Lower hauling rope Uphill ride**	**Lower hauling rope Downhill ride**
Minimum gradient [U/100m]	-0.36	0.08	-1.92	-0.31
Average gradient [U/100m]	**-0.12**	**0.44**	**-0.75**	**0.14**
Maximum gradient [U/100m]	0.20	1.08	-0.06	1.06
Absolute Rotations min [U]	-8.00	-7.00	-12.00	-9.00
Absolute Rotations Aver. [U]	**-1.00**	**3.64**	**-4.92**	**-4.00**
Absolute Rotations max [U]	9.00	11.00	9.00	3.00

4 Lay length analysis of filtered magneto-inductive rope-tests

At a first glance, the ground signal of an MRT appears to contain no useful information. For this reason it is sometimes misleadingly called ground “noise” instead of “signal” as a much better expression. Any damage signal like e.g. wire breaks or lightning strokes peak out of the signal basis as a characteristic signal which has to be interpreted by the inspector in charge [Per16]. Invisible to the human eye are those periodic frequencies of the strand and rope lay length, which are also carried by the ground signal [Wid13]. By local Fourier transformation in sections of the measurement, it is possible to display a lay length chart over the whole rope length at the measuring point – which is in general directly at the station, close to sheaves and drive pulleys reducing the ropes residual life time by every bending cycle.

Carrying out local Fourier analysis creates some problems which have to be solved by additional tools. E.g. the edges of each frame of local analysis cause discontinuities which can be suppressed by a so-called Hamming-window, which allows fading out the intensity of the perturbing border area. In the final evaluation model, the deviation of lay length can be directly related to the twist angle and thus the resulting lifetime (reduction) of the bending tests. For this purpose, the following equation is used describing the lay angel β‘ in twisted state given by [Ern12]:

$$\tan \beta' = \frac{\tan \beta - R\omega}{1 + \varepsilon_D}$$

DOI: 10.2195/lj_NotRev_kuehner_en_201803_01
URN: urn:nbn:de:0009-14-46707

β'	lay angle of the twisted rope [rad]
R	pitch radius of the strands [mm]
ω	length related twist angle [rad/mm]
ε_D	wire elongation

The equation is slightly modified by neglecting the wire elongation ε_D and substituting the twisted lay angle for the change of lay length in twisted state:

$$\omega = \frac{\tan\beta}{R} \cdot \left(1 - \frac{L_L}{L_L{}'}\right)$$

L_L	nominal lay length [mm]
L_L'	lay length in twisted state [mm]

The formula could be proved by the experimental results comparing applied twist angle and resulting lay length in the bending tests. Doing this, the first focal points of the project are successfully joined. It is now possible to relate the expectable lifetime to the measured lay length at the twisted portions of the rope.

Following, typical shapes of lay length charts of upper and lower hauling ropes are given in figure 9. In general, upper hauling ropes show a convex lay length shape, de-twisting in their middle sections and closing at the edges. Instead, lower hauling ropes show a concave lay length chart with closing twist in the middle sections and de-twisting at their edges.

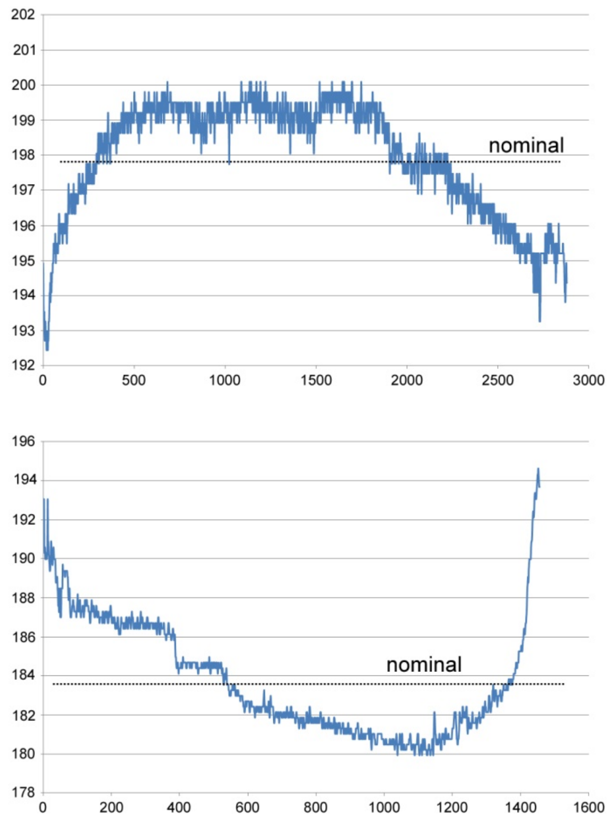

Figure 9. Typical shapes of lay length charts of upper (top) and lower hauling ropes (bottom) (x-axis: rope distance [m], y-axis: lay length [mm])

The range of calculated twist angles based on the lay length extracted of the MRT-measurements is given in table 4.

Table 4. Range of calculated twist angles in middle sections and at edges (positive: closing twist, negative: de-twisting)

	Upper hauling ropes, edge	**Upper hauling rope, middle section**
Minimum twist angle [°/100d]	--	-162.2
Average twist angle [°/100d]	92.9	-72.0
Maximum twist angle [°/100d]	312.8	--
	Lower hauling ropes, edge	**Lower hauling rope, middle section**
Minimum twist angle [°/100d]	-487.7	--
Average twist angle [°/100d]	-231.0	83.7
Maximum twist angle [°/100d]	--	151.0

5 COMBINED MODEL

The identified, analysed and developed influencing factors are set into relation within a combined model. At first, different possible methods are analysed and tested for efficiency and suitability:

- Rating following VDI 2225 [Fel13],[VDI2225]
- Polynomial of similar structure to lifetime formula by Feyrer [Fey00]
- Linear damage hypothesis of Palmgren-Miner [Pal24]
- (Economical) decision theories of e.g. Hurwicz or Savage-Niehans [Bam12]

By evaluating the methods referring to specially raised criteria like traceability, flexibility and functionality of the final model, a joined formula of both technical rating and damage hypothesis of Palmgren-Miner was developed. The formula for the reference reduction level Φ_{ref} caused by

DOI: 10.2195/lj_NotRev_kuehner_en_201803_01
URN: urn:nbn:de:0009-14-46707

twist is expressed as follows, using the backgrounds of these factors developed within the FMEA:

- No.01: diameter related height force S_H/d^2
- No.02: diameter related friction force S_R/d^2 caused by change of travelling direction
- No.05: diameter related traction drive force S_U/d^2
- No.08: diameter related torque caused by tower friction M_{ST}/d
- No.09: diameter related torque caused by slack hanger friction M_{SR}/d.

$$\Phi_{ref} = \left(\frac{\frac{S_{H,j}}{d_j^2} \cdot f_{01}}{69{,}9 \frac{N}{mm^2}} + \frac{\frac{S_{R,j}}{d_j^2} \cdot f_{02}}{23{,}3 \frac{N}{mm^2}} + \frac{\frac{S_{U,j}}{d_j^2} \cdot f_{05}}{96{,}1 \frac{N}{mm^2}} + \frac{\frac{M_{ST,j}}{d_j} \cdot f_{08}}{0{,}426 \frac{Nm}{mm}} + \frac{\frac{M_{SR,j}}{d_j} \cdot f_{09}}{1{,}113 \frac{Nm}{mm}} \right) \cdot \frac{1}{\sum f_i}$$

For validation, the equation is linked to the actual normalized states of twisted lay length, residual rope lifetime and rotation difference between up- and downhill ride. Achieving a value of 100% means that the rope will show the maximum lifetime reduction level by twist which has been revealed in the quantity of investigated ropeway systems. Using values of the database generated within this project, the final equation for the damage level Φ_{act} of the actual side is:

$$\Phi_{act,i} = \left[\frac{\omega_j}{-487{,}7°/100d} \cdot 1 + \left(1 - \frac{\frac{Z_{Am,IST,j}}{Z_{Am,Fey,j}}}{3{,}274} \right) \cdot 0{,}5 + \frac{19 - \Delta N_{rot,B-T,j}}{42} \cdot 1 \right] \cdot \frac{1}{2{,}5}$$

Φ	damage level [%]
ω	length related twist angle [°/m]
f	factor for technical rating [-]
ZAm	rope life time referring to discard maturity of 50 % of the ropes [cycles]
N	turns of the rope within an up- and downhill ride cycle [U]

The necessary rating factors $f_{i,j}$ of the reference level have been separated to different sets for upper and lower hauling ropes, differentiating direct influence of and isolation against the traction drive. This was done referring to the different lay length characteristics of the four different combinations. The factors were optimized keeping whole-number values to strengthen the convenience of using the model for third parties. Also the risk of errors e.g. by mistyping is lowered by this strategy. Negative values are also permitted to allow the influencing factors a positive effect on the twist behavior as it is demanded in the literature [Eng77]. The best fit parameter sets are given in the following table 5.

Table 5. Parameter sets for analysing the reference level of damage Φ_{ref}

Factor $f_{i,j}$	**01**	**02**	**05**	**08**	**09**
Upper hauling rope with drive	2	3	1	3	2
Upper hauling rope	1	2	0	0	-1
Lower hauling rope with drive	1	1	3	-1	1
Lower hauling rope	2	3	-2	0	1

The quality of the final model can be expressed by the average deviation between calculated damage of the reference side and the actual damage developed using the data basis of existing ropeway systems. The achieved value of average deviation is -1.61 %. The referring standard deviation of this level is 16.3 %, which may appear high in mathematical terms. But for (experimental) rope research applications, deviations below 20 % can be rated as a satisfying range.

6 Adaptivity to other Rope Drives

Within the project, the adaptivity of the findings to other rope drives shall be evaluated. A first step is made following the rotation behavior of continuous moving gondola systems which show a free rotating closed rope loop without fixed ends – if the vehicles are taken off the rope. The theoretical rotation analysis can be adapted using a modified master data sheet. Although the rotation does not result in residual twist and thus not affect the ropes lifetime, the analysis and measurements can help to evaluate the correctness of track gauge adjustment. In addition, eliminating torque multipliers can reduce operational vibration of the system. For future research, advice is given on implementing rotation analysis in general rope drive environments, taken into concern common rope design varieties and drive setups as well as alternative materials like high modulus fibre ropes. Existing literature on torque and twist is sorted to common subjects to support future research.

7 Conclusions

The research project on rope rotation, residual twist and resulting lifetime reduction of ropeway ropes allows an approach to analyse a ropeway system regarding its geometrical setup and technical equipment for the first time. The results show a severe influence of rotation on the serviceable rope life time by the conducted bending tests. In addition, the field-test data of measured residual lay length and digital rope rotation measurements revealed that rotation and twist characteristics of the ropes running in rope drives are repeatable and comprehensive. The final model allows calculating the expectable damage level caused by rope twist with a high average performance and a satisfying standard deviation. With an increasing database integrating input of third party users, the models values can be refreshed continuously to fit to future developments in rope design and ropeway techniques.

In the future, the experiences made in this project can be transferred to investigation of general rope drives and their individual rotational problems.

In addition to the project report of the German research association DFG, project no. WE 2187/36-1, a PhD thesis written in german language can be downloaded at the library of University of Stuttgart, giving further details on the project steps, intermediate results and conclusions [Kue17].[5]

Literature

[Bam12] Bamberg, G. et. al.: Betriebswirtschaftliche Entscheidungslehre. 15. Aufl., Vahlen-Verlag, München 2012

[Bri95] Briem, U.: Bruchkraftverlust bei Verschleiß durch Litzenberührung. In: DRAHT (46), S. 517–521, Meisenbach Verlag, 1995

[DIN12927] Norm DIN EN 12927-7, 06-2005: Sicherheitsanforderungen für Seilbahnen für den Personenverkehr, Seile, Teil 7: Inspektion, Reparatur und Wartung.

[Ebe13] Eberhardt, O.: Risikobeurteilung mit FMEA. Die Fehlermöglichkeits- und Einfluss-Analyse gemäß VDA-Richtlinie 4.2, 3rd edition, expert Verlag, Renningen 2013

[Eng77] Engel, E.: Über den Laufwiderstand gefütterter Seilrollen. Institutsheft Nr. 6, Hg. v. Institut für Eisenbahnwesen, Verkehrswirtschaft und Seilbahnen, Technische Universität Wien 1977

[Eng94] Engel, E.: Drall-Verfrachtung bei Zugseilen. Hg. v. Institut für Eisenbahnwesen, Verkehrswirtschaft und Seilbahnen, Institutsheft 21, TU Wien 1994

[Ern12] Ernst, B.: Zum Einfluss von Verdrehungen auf die Eigenschaften zugschwellbelasteter Drahtseile. PhD thesis. Institute of Mechanical Handling and Logistics (IFT), University of Stuttgart 2012

[Fel13] Feldhusen, J.; Grote, K.-H. (Hrsg.): Pahl/Beitz Konstruktionslehre. Methoden und Anwendung erfolgreicher Produktentwicklung. 8th edition, Springer-Verlag, Wien 2013

[Fey00] Feyrer, K.: Drahtseile. Bemessung, Betrieb, Sicherheit. 2nd edition, Springer-Verlag, Wien 2000

[ITT15] I.T.T.A.B.: Summary of Statistics. International Tagung der technischen Aufsichtsbhörden (I.T.T.A.B.), Bariloche/Argentinien 2015

[Kue17] Kühner, K.: Beitrag zur Beurteilung der Schädigung von Seilbahnseilen durch Drehung und Verdrehung im Betrieb. PhD thesis. Institute of Mechanical Handling and Logistics (IFT), University of Stuttgart 2017

[Opl04] Oplatka, G.: Drall in Zug- und Förderseilen. In: Internationale Berg- und Seilbahnrundschau (ISR) Nr. 05/2004, Bohmann Verlag, Wien 2004

[Pal24] Palmgren, A.: Die Lebensdauer von Kugellagern. In: Zeitschrift des Vereins Deutscher Ingenieure 68, 05.04.1924, S. 339–341, VDI-Verlag, Berlin 1924

[Per16] Pernot, S. et. al.: Survey on Magnetic Rope Testing. OITAF Book No 3., Bozen 2016

[Web13] Weber, T.: Beitrag zur Untersuchung des Lebensdauerverhaltens von Drahtseilen unter einer kombinierten Bean-

[5] download link: https://elib.uni-stuttgart.de

spruchung aus Zug, Biegung und Torsion. PhD thesis. Institute of Mechanical Handling and Logistics (IFT), University of Stuttgart 2013

[Weh13] Wehking, K.-H.; Kühner, K. ; Winter, S.: Dem Seildrall auf der Spur. In: Internationale Seilbahnrundschau 01/2013, Bohmann Verlag, Wien 2013

[Wid13] Widmann, M.: Analyse von magnetinduktiven Seilprüfsignalen. Studienarbeit (seminar paper), Institute of Mechanical Handling and Logistics (IFT), University of Stuttgart 2013

[VDI2225] Richtlinie VDI 2225-3, 11-1998: Konstruktionsmethodik, Technisch-wirtschaftliches Konstruieren, Blatt 3: Technisch-wirtschaftliche Bewertung.

Dr.-Ing. Konstantin Kühner, Research & Development, Rope and Lifting Technology at Jakob AG. Konstantin Kuehner was born in 1983 in Siegen, Germany. Between 2009 and 2017 he worked as a ropeway expert and research assisteant at IFT University of Stuttgart. Since Summer 2017 he has been working at the Jakob AG.

Address: Jakob AG, Dorfstrasse 34, CH-3555 Trubschachen, Swiss,
Phone: +41 34 495 1010, Fax: +41 34 495 1025,
E-Mail: konstantin.kuehner@jakob.eu

Unv.-Prof. Dr.-Ing. Dr. h. c. Karl-Heinz Wehking, head of Institute of Mechanical Handling and Logistics (IFT), University of Stuttgart. Karl-Heinz Wehking has been leading IFT in Stuttgart since 1995. Since 2006, he is acting as vice president of the intra-logistics network of the county Baden-Württemberg e.V. He was nominated honorary doctor by the States Polytechnical University of Odessa in 2012.

Address: IFT Universität Stuttgart, Holzgartenstraße 15B, D-70174 Stuttgart, Germany,
Phone: +49 711 685 83770, Fax: +49 711 685 83769,
E-Mail: wehking@ift.uni-stutgart.de